5820 *Inorg. Chem.* **2009**, *48*, 5820–5828
DOI: 10.1021/ic900003m

Inorganic Chemistry
Article

Hetero-Metallic {3d-4f-5d} Complexes: Preparation and Magnetic Behavior of Trinuclear [(L^{Me2}Ni−Ln){W(CN)$_8$}] Compounds (Ln = Gd, Tb, Dy, Ho, Er, Y; L^{Me2} = Schiff base) and Variable SMM Characteristics for the Tb Derivative

Jean-Pascal Sutter,*[†,‡] Sébastien Dhers,[†,‡] Raghunathan Rajamani,[§] S. Ramasesha,*[§] Jean-Pierre Costes,[†,‡] Carine Duhayon,[†,‡] and Laure Vendier[†,‡]

[†]*CNRS, Laboratoire de Chimie de Coordination (LCC), 205, route de Narbonne, F-31077 Toulouse, France,* [‡]*Université de Toulouse, UPS, INPT, LCC, F-31077 Toulouse, France, and* [§]*Solid State and Structural Chemistry Unit, Indian Institute of Science, Bangalore 560012, India*

Received January 2, 2009

Assembling bimetallic {Ni−Ln}$^{3+}$ units and {W(CN)$_8$}$^{3-}$ is shown to be an efficient route toward heteronuclear {3d-4f-5d} compounds. The reaction of either the binuclear [{L^{Me2}Ni(H$_2$O)$_2$}{Ln(NO$_3$)$_3$}] complexes or their mononuclear components [L^{Me2}Ni] and Ln(NO$_3$)$_3$ with (HNBu$_3$)$_3${W(CN)$_8$} in dmf followed by diffusion of tetrahydrofuran yielded the trinuclear [{L^{Me2}NiLn}{W(CN)$_8$}] compounds **1** (Ln = Y), **2a,b** (Gd), **3a,b** (Tb), **4** (Dy), **5** (Ho), and **6** (Er) as crystalline materials. All of the derivatives possess the trinuclear core resulting from the linkage of the {W(CN)$_8$} to the Ni center of the {Ni−Ln} unit. Differences are found in the solvent molecules acting as ligands and/or in the lattice depending on the crystallization conditions. For all the compounds ferromagnetic {Ni−W} and {Ni−Ln} (Ln = Gd, Tb, Dy, and Er} interactions are operative resulting in high spin ground states. Parameterization of the magnetic behaviors for the Y and Gd derivatives confirmed the strong cyano-mediated {Ni−W} interaction (J_{NiW} = 27.1 and 28.5 cm^{-1}) compared to the {Ni−Gd} interaction (J_{NiGd} = 2.17 cm^{-1}). The characteristic features for slow relaxation of the magnetization are observed for two Tb derivatives, but these are modulated by the crystal phase. Analysis of the frequency dependence of the alternating current susceptibility data yielded U_{eff}/k_B = 15.3 K and $\tau_0 = 4.5 \times 10^{-7}$ s for one derivative whereas no maxima of χ_M'' appear above 2 K for the second one.

Introduction

The construction of supramolecular magnetic materials by association of two different paramagnetic metal ions, that is, the bimetallic approach,[1−4] has been a major breakthrough allowing rapid development of molecule-based magnets and more recently of single molecule/chain magnets. Rather surprisingly, the use of more complex units, for instance bi- or poly metallic units, as building blocks is a much less explored route. The latter, however, presents the opportunity to design original materials with building units possessing properties not exhibited by single ions (such as large spin ground state and slow relaxation of the magnetization, etc.).[5−7] This approach also provides a route toward ternary materials, that is, compounds involving three different ions as exchange coupled spin carriers. We report here on a series of heterometallic {3d-4f-5d} compounds obtained by this route.

Our interest in heteronuclear {3d-4f} compounds results from the slow relaxation of the magnetization they may exhibit for Ln ions with strong spin−orbit coupling.[8−10] It has been shown that a simple bimetallic {Cu−Tb} compound possesses the characteristic features of a single molecule magnet.[11,12] To achieve species of larger nuclearity and hence improved magnetic behavior, we have envisaged assembling

*To whom correspondence should be addressed. E-mail: sutter@lcc-toulouse.fr (J.-P.S.), ramasesh@sscu.iisc.ernet.in (S.R.).

(1) Kahn, O. *Molecular Magnetism*; VCH: Weinheim, 1993.
(2) Verdaguer, M.; Bleuzen, A.; Marvaud, V.; Vaissermann, J.; Seuleiman, M.; Desplanches, C.; Sciuller, A.; Train, C.; Garde, R.; Gelly, G.; Lomenech, C.; Rosenman, I.; Veillet, P.; Cartier, C.; Villain, F. *Coord. Chem. Rev.* **1999**, *190−192*, 1023–1047.
(3) Kahn, O. *Acc. Chem. Res.* **2000**, *33*, 647–657.
(4) Mathonière, C.; Sutter, J.-P.; Yakhmi, J. V. Bimetallic magnets: Present and perspectives. In *Magnetism: molecules to materials*; Miller, J. S., Drillon, M., Eds.; Wiley-VCH: Weinheim, 2002; Vol. 4, pp 1−40.
(5) Miyasaka, H.; Yamashita, M. *Dalton Trans.* **2007**, 399–406.
(6) Roubeau, O.; Clérac, R. *Eur. J. Inorg. Chem.* **2008**, 4325–4342.
(7) Branzea, D.; Sorace, L.; Maxim, C.; Andruh, M.; Caneschi, A. *Inorg. Chem.* **2008**, *47*, 6590–6592.
(8) Ishikawa, N.; Sugita, M.; Ishikawa, T.; Koshihara, S.; Kaizu, Y. *J. Am. Chem. Soc.* **2003**, *125*, 8694–8695.
(9) Osa, S.; Kido, T.; Matsumoto, N.; Re, N.; Pochaba, A.; Mrozinski, J. *J. Am. Chem. Soc.* **2004**, *126*, 420–421.
(10) Ishikawa, N.; Sugita, M.; Wernsdorfer, W. *Angew. Chem., Int. Ed.* **2005**, *44*, 2931–2935.
(11) Costes, J. P.; Dahan, F.; Wernsdorfer, W. *Inorg. Chem.* **2006**, *45*, 5–7.
(12) Kajiwara, T.; Nakano, M.; Takaishi, S.; Yamashita, M. *Inorg. Chem.* **2008**, *47*, 8604–8606.

 Published on Web 06/04/2009

such bimetallic units into larger supramolecular objects by means of a complementary building unit in such a way that it also ensures efficient ferro/ferri-magnetic interaction among the magnetic units.[13] The 5d complex $\{W(CN)_8\}^{3-}$ was chosen as the assembling unit because such octacyanometallates can accommodate several larger metal complexes[14−18] and especially because of the rather strong exchange interactions that take place with the 3d ions linked to the cyanide ligands. It has been established that the interaction with Ni(II) is ferromagnetic[13,19−22] with a magnitude about one order larger than the {3d-4f} interaction. Hence, the assemblage of bimetallic {Ni−Ln} units and $\{W(CN)_8\}^{3-}$ appear at the outset to be an interesting combination.

In this report we disclose a series of compounds resulting from assembling $\{Ni-Ln\}^{3+}$ units (Ln = Y, Gd, Tb, Dy, Ho, and Er) and $\{W(CN)_8\}^{3-}$ in dimethylformamide (dmf). This solvent permitted the formation of strictly trinuclear {Ni−Ln−W} species, which allowed an accurate investigation of the exchange interactions operative between the spin carriers. Interestingly, the characteristic features of slow relaxation of the magnetization have been found to be different for two trinuclear {Ni−Tb−W} derivatives with distinct solvent composition and crystal packing.

Results and Discussion

Synthesis and Crystal Structures. The reaction of either the binuclear $[\{L^{Me2}Ni(H_2O)_2\}\{Ln(NO_3)_3,\}]$ complexes (Chart 1) or their mononuclear components $[L^{Me2}Ni]$ and $Ln(NO_3)_3$, with $(HNBu_3)_3\{W(CN)_8\}$ followed by diffusion of tetrahydrofuran (THF) yielded the trinuclear $[\{L^{Me2}NiLn\}\{W(CN)_8\}]$ compounds **1** (Ln = Y), **2a,b** (Gd), **3a,b** (Tb), **4** (Dy), **5** (Ho), and **6** (Er) as crystalline materials. All of the derivatives possess the trinuclear core resulting from the linkage of the $\{W(CN)_8\}$ to the Ni center of the {Ni−Ln} unit (Figure 1−4). Differences are found in the solvent molecules acting as ligands and/or in the lattice, depending on the crystallization conditions. Synthesis in anhydrous dmf led to the crystalline compounds **1** (Y), **2a** (Gd), **3a** (Tb), **4** (Dy), and **5** (Ho) of formula $[\{L^{Me2}Ni(dmf)Ln(dmf)_4\}\{W(CN)_8\}]\cdot H_2O$ (2 H_2O for **5**, or 0.5 dmf for **3a**)[23] whereas crystallization in dmf containing H_2O yielded $[\{L^{Me2}Ni(dmf)Gd(dmf)_3(H_2O)\}\{W(CN)_8\}]\cdot H_2O\cdot 0.5THF\cdot 0.5dmf$, **2b**, $[\{L^{Me2}Ni(H_2O)Tb(dmf)_{2.5}(H_2O)_{1.5}\}\{W(CN)_8\}]\ H_2O\cdot 0.5dmf$, **3b**, and $[\{L^{Me2}Ni(H_2O)Er(dmf)_3(H_2O)\}\{W(CN)_8\}]\cdot H_2O\cdot 0.5dmf$, **6**. Single crystals suitable for X-ray diffraction studies have been obtained for all compounds except **2a**. The structures have been solved for **2b**, **3a,b**, **4**, **5**, and **6**, and cell parameters have been recorded for **1** (Experimental Section).

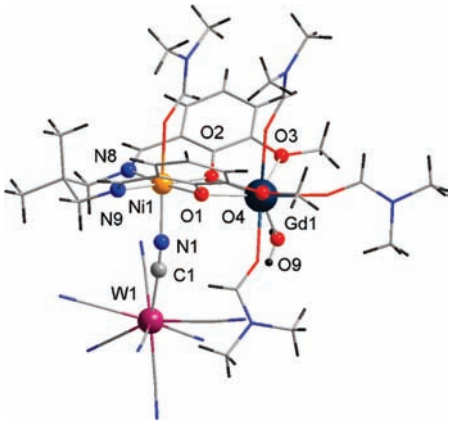

Figure 1. $[L^{Me2}Ni(dmf)Gd(dmf)_3(H_2O)\{W(CN)_8\}]\cdot H_2O\cdot 0.5THF\cdot 0.5$-dmf, **2b**. Selected interatomic distances (Å) and angles (deg): Ni−N1, 2.071(5); Ni−N8, 2.006(4); Ni−N9, 2.008(4); Ni−O1, 2.006(3), Ni−O2, 2.018(3); Ni−O8(dmf), 2.178(3); Gd−O1, 2.314(3); Gd−O2, 2.306(3); Gd−O3, 2.594(4); Gd−O4, 2.607(4); Gd−O9, 2.407(4); Gd−O(dmf), 2.279(4)−2.337(4); Ni···Gd, 3.405(1); Ni−N1−C1, 161.2(4)°; dihedral angle between the planes defined by O1−Ni−O2 and O1−Gd−O2, 8.1(1)°.

Chart 1. Schematic View of the Ligand and Complexes Involved in the Preparation of the Trinuclear Compounds

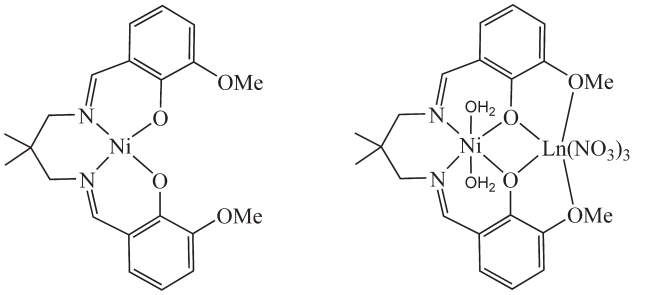

$\{L^{Me2}Ni\}$ $[\{L^{Me2}Ni(H_2O)_2\}\{Ln(NO_3)_3\}]$

The molecular structures for compounds **2b**, **3b**, **4**, and **6** are depicted in the Figures 1 to 4 with selected geometrical data; ORTEP plots of the related asymmetric units, as well as for **3a** and **5**, are given as Supporting Information. All compounds exhibit a trinuclear core made by association of a $\{W(CN)_8\}$ moiety and a $\{L^{Me2}NiLn\}$ unit by means of CN linkage to the Ni ion. The Ni ion is in an elongated octahedral surrounding which is realized by the equatorial coordination of the Schiff-base ligand, the axial positions being occupied by the bridging cyanide and a solvent molecule, that is, dmf for **2b**, **3a**, **4**, and **5**, H_2O for **3b** and **6**. The coordination sphere of the Ln ion accommodates four O from L^{Me2} and four solvent molecules, that is, 3 dmf and 1 H_2O for **2b** and **6**; 2.5 dmf and 1.5 H_2O for **3b**; 4 dmf for **3a**, **4**, and **5**. The Ni←NC bond lengths are comprised between 2.021 and 2.094 Å, the angles are 161.2(4)° (**2b**), 155.5(4) (**3a**), 166.9(5)° (**3b**), 153.3(8)° (**4**) 154.8(3) (**5**), and 167.0(3)° (**6**). It can be noticed that the deviation from linearity increases with

(13) Sutter, J.-P.; Dhers, S.; Costes, J.-P.; Duhayon, C. *C.R. Chimie* **2008**, *11*, 1200–1206.
(14) Sieklucka, B.; Podgajny, R.; Przychodzen, P.; Korzeniak, T. *Coord. Chem. Rev.* **2005**, *249*, 2203–2221.
(15) Lim, J. H.; Yoon, J. H.; JKim, H. C.; Hong, C. S. *Angew. Chem., Int. Ed.* **2006**, *45*, 7424–7426.
(16) Zhao, H.; Shatruk, M.; Prosvirin, A. V.; Dunbar, K. R. *Chem.—Eur. J.* **2007**, *13*, 6573–6589.
(17) Venkatakrishnan, T. S.; Rajamani, R.; Ramasesha, S.; Sutter, J. P. *Inorg. Chem.* **2007**, *46*, 9569–9574.
(18) Venkatakrishnan, T. S.; Imaz, I.; Sutter, J. P. *Inorg. Chim. Acta* **2008**, *361*, 3710–3713.
(19) Bonadio, F.; Gross, M.; Stoeckli-Evans, H.; Decurtins, S. *Inorg. Chem.* **2002**, *41*, 5891–5896.
(20) Visinescu, D.; Desplanches, C.; Imaz, I.; Bahers, V.; Pradhan, R.; Villamena, F.; Guionneau, P.; Sutter, J. P. *J. Am. Chem. Soc.* **2006**, *128*, 10202–10212.
(21) Withers, J. R.; Li, D.; Triplet, J.; Ruschman, C.; Parkin, S.; Wang, G.; Yee, G. T.; Holmes, S. M. *Polyhedron* **2007**, *26*, 2353–2366.
(22) Nowicka, B.; Rams, M.; Stadnicka, K.; Sieklucka, B. *Inorg. Chem.* **2007**, *46*, 8123–8125.
(23) Note: other crystals of **3a** obtained in the same conditions gave cell parameters (α = 11.99, β = 26.18, γ = 19.44 Å, β = 106.53°, V = 5540 Å^3) very similar to those of **4** suggesting that the Tb derivative may crystallize with either dmf or H_2O as lattice molecules.

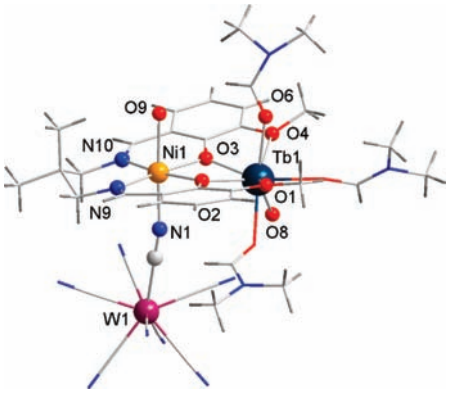

Figure 2. Molecular structure for $[L^{Me2}Ni(H_2O)Tb(dmf)_{2.5}(H_2O)_{1.5}\{W(CN)_8\}]\cdot H_2O\cdot 0.5dmf$, **3b**. One of the depicted dmf bound to Tb has occupation 1/2, the O6 being common with H_2O found in the absence of the dmf unit. Selected interatomic distances (Å) and angles (deg): Ni−N1, 2.069(5); Ni−N9, 2.029(5); Ni−N10, 2.016(5); Ni−O2, 2.024(4), Ni−O3, 2.031(4); Ni−O9, 2.150(6); Tb−O1, 2.588(5); Tb−O2, 2.300(4); Tb−O3, 2.279(4); Tb−O4, 2.578(4); Tb−O6, 2.328(4); Tb−O8, 2.333(5); Tb−O (dmf), 2.303(5)−2.332(5); Ni···Tb, 3.455(1); Ni−N1−C1, 166.9(5)°; dihedral angle between the planes defined by O2−Ni−O3 and O2−Tb−O3, 14.8(1)°.

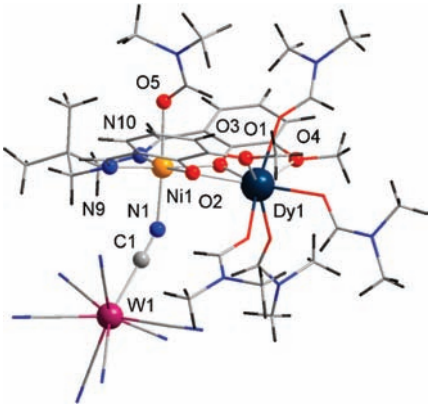

Figure 3. $[L^{Me2}Ni(dmf)Dy(dmf)_4\{W(CN)_8\}]\cdot H_2O$, **4**; the same trinuclear moiety applies for Tb and Ho derivatives **3a** and **5**. Selected interatomic bond distances (Å) and angles (deg) for **4/3a/5**: Ni−N1, 2.094(9)/2.083(4)/2.097(3); Ni−N9, 2.010(9)/2.029(4)/2.021(3); Ni−N10, 2.001(8)/1.997(4)/1.997(3); Ni−O2, 2.023(6)/2.031(3)/2.026(3), Ni−O3, 2.028(7)/2.021(3)/2.012(3); Ni−O5, 2.184(9)/2.141(4)/2.152(3); Ln−O1, 2.605(8)/2.589(4)/2.564(3); Ln−O2, 2.287(8)/2.289(4)/2.272(3); Ln−O3, 2.279(6)/2.289(3)/2.275(3); Ln−O4, 2.641(7)/2.643(4)/2.622(3); Ln−O (dmf), 2.24(1)−2.35(1)/2.266(4)−2.370(4)/2.253(4)−2.331(3); Ni···Ln, 3.411(1)/3.4244(6)/3.4068(5); Ni−N1−C1, 153.3(8)/155.5(4)/1.548(3)°; dihedral angle between the planes defined by O2−Ni−O3 and O2−Ln−O3, 13.8(3)/13.7(1)/12.8(1)°.

the number of dmf in the coordination sphere of the Ln ion suggesting a bending due to steric crowding. Conversely the ligand trans to the cyanide (H_2O versus dmf) has no incidence on the Ni←N bond characteristics. The geometry of the $\{W(CN)_8\}$ fragment has been analyzed with the SHAPE program[24] revealing a slightly distorted square antiprismatic shape for all compounds;[25] the results are tabulated in the Supporting Information. The crystal lattices of all compounds contain solvents

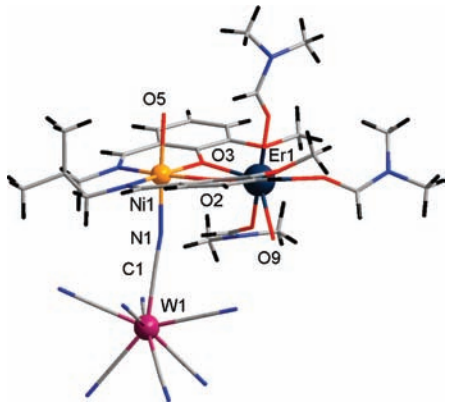

Figure 4. Molecular structure for $[L^{Me2}Ni(H_2O)Er(dmf)_3(H_2O)\{W(CN)_8\}]\cdot H_2O\cdot 0.5dmf$, **6**. Selected interatomic bond distances (Å) and angles (deg): Ni−N1, 2.067(3); Ni−N9, 2.016(3); Ni−N10, 2.017(3); Ni−O5, 2.139(4); Ni−O2, 2.029(3); Ni−O3, 2.019(3); Er−O2, 2.249(3); Er−O3, 2.266(3); Er−O9, 2.305(4); Er−O(dmf), 2.268(4)−2.289(4); Ni···Er, 3.4268(5) Å; Ni−N1−C1, 167.0(3)°; dihedral angle between the planes defined by O2−Ni−O3 and O2−Er−O3, 14.37(7)°.

molecules, some with partial occupation (for **2b**, **3a,b**, **6**, see Experimental Section) or disordered (**5**), leading to the formulations given above. The shortest separation between paramagnetic ions of neighboring molecules are for **2b** 7.9244(3) Å (W−Gd) and 10.2619(7) Å (W−Ni), for **3a** 8.732(1) (W−Tb) and 8.778(1) (W−Ni), for **3b** 7.370(1) Å (W−Tb) and 8.767(1) Å (W−Ni), and for **4** 8.754(1) Å (Dy−W) and 8.815(2) Å (Ni−W). Finally, the cell parameters recorded for **1** (Experimental Section) unambiguously established that this derivative is isomorphous to **3a**, **4**, and **5**.

Magnetic Properties. Static Magnetic Susceptibility. The magnetic behavior for the compounds has been investigated in the temperature domain 2−300 K on polycrystalline samples held in grease in an applied field of 1000 Oe. The temperature dependence of the product of the molar magnetic susceptibilities, χ_M, and temperature are shown in Figures 5 and 6. For all the compounds the $\chi_M T$ product at 300 K (1.48 (**1**), 9.36 (**2a**), 13.17 (**3a**, see Supporting Information), 13.30 (**3b**), 15.45 (**4**), 15.6 (**5**); 12.87 $cm^3\ mol^{-1}\ K$ (**6**)) is in agreement with the paramagnetic contribution of components ({W(V), 0.375 $cm^3\ mol^{-1}\ K$; Ni(II), 1.1 $cm^3\ mol^{-1}\ K$; Gd(III), 7.88 $cm^3\ mol^{-1}\ K$; Tb(III), 11.81 $cm^3\ mol^{-1}\ K$; Dy(III), 14.10 $cm^3\ mol^{-1}\ K$; Ho(III), 14.07 $cm^3\ mol^{-1}\ K$; Er(III), 11.48 $cm^3\ mol^{-1}\ K$). In the low temperature domain an increase of $\chi_M T$ is observed revealing the occurrence of ferromagnetic interactions for all the compounds except **5**. For compound **1**, only the exchange interaction between the W and the Ni centers is operative, the Y(III) being diamagnetic. The observed behavior is in agreement with the ferromagnetic W−CN−Ni interaction previously reported.[13,19−22] For the Gd derivative **2a**, both the Ni−W and Ni−Gd interactions are anticipated to be ferromagnetic.[26,27] The maximum value for $\chi_M T$, 12.1 $cm^3\ mol^{-1}\ K$, is indeed close to the value anticipated (15 $cm^3\ mol^{-1}\ K$) for an $S = 5$ state. For the Tb, Dy, and Er compounds the ferromagnetic interaction with Ni is

(24) Llunell, M.; Casanova, D.; Cirera, J.; Bofill, J. M.; Alemany, P.; Alvarez, S.; Pinsky, M.; Avnir, D. *SHAPE: Continuous shape measures of polygonal and polyhedral molecular fragments*, 1.1b; University of Barcelona: Barcelona, 2005.

(25) Casanova, D.; Llunell, M.; Alemany, P.; Alvarez, S. *Chem.—Eur. J.* **2005**, *11*, 1479–1494.

(26) Costes, J. P.; Dahan, F.; Dupuis, A.; Laurent, J.-P. *Inorg. Chem.* **1997**, *36*, 4284–4286.

(27) Costes, J. P.; Donnadieu, B.; Gheorghe, R.; Novitchi, G.; Tuchagues, J. P.; Vendier, L. *Eur. J. Inorg. Chem.* **2008**, 5235–5244.

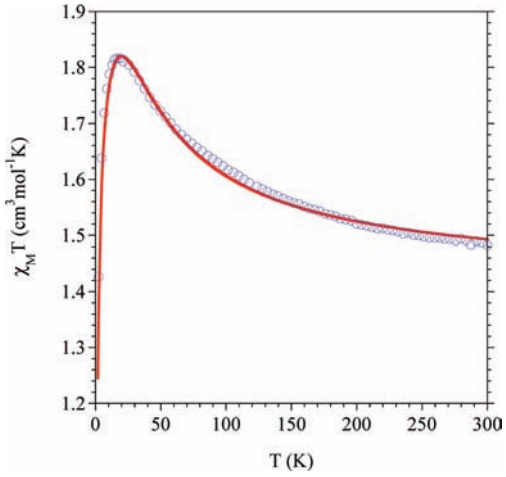

Figure 5. Experimental (○) and calculated (solid line) temperature dependence of $\chi_M T$ for **1**. Best fit parameters: J_{NiW} = 28.5 cm^{-1}, D_{Ni} = 0.44 cm^{-1}, zJ' = −0.51 cm^{-1}, g = 2.02 (see text).

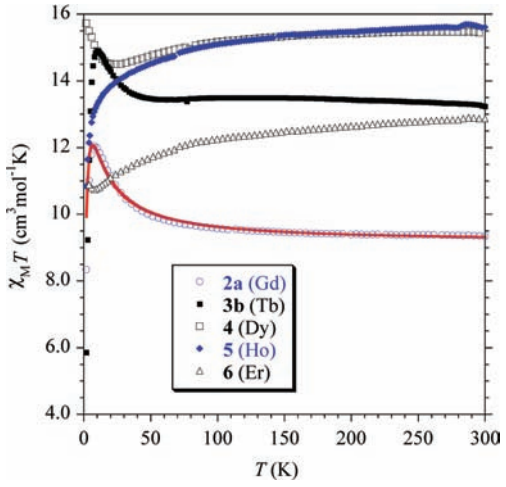

Figure 6. Temperature dependence of $\chi_M T$ for **2a** (○), **3b** (■), **4** (□), **5** (◆), and **6** (Δ). The solid line is the calculated behavior for the Gd derivative yielding J_{NiW} = 27.1 cm^{-1}, J_{NiGd} = 2.17 cm^{-1}, D_{Ni} = 0.5 cm^{-1}, zJ' = −0.06 cm^{-1}, g = 2.0 (see text).

clearly supported by the increase of $\chi_M T$ below 50 K.[28] The slight decrease of $\chi_M T$ occurring in the intermediate temperature domain for **3a,b**, **4**, and **6** is attributed to the intrinsic behavior of the anisotropic Ln ions.[29−31] For the Ho derivative this effect leads to a decrease for $\chi_M T$ of much larger amplitude,[29] hence masking the expected ferromagnetic {Ni−Ho} interaction. [28] The field dependence of the magnetizations recorded at 2 K (Figure 7) confirm the occurrence of ferromagnetic interactions between the metal ions with magnetization values at 5 T close to those anticipated for the respective spin ground states (e.g., S = 3/2 for **1**, S = 5 for **2a**). It can be noticed, however, that saturation is not reached. For the diamagnetic Y (**1**) and isotropic Gd (**2a**) derivatives, this is attributed to the anisotropy of the Ni ion in distorted

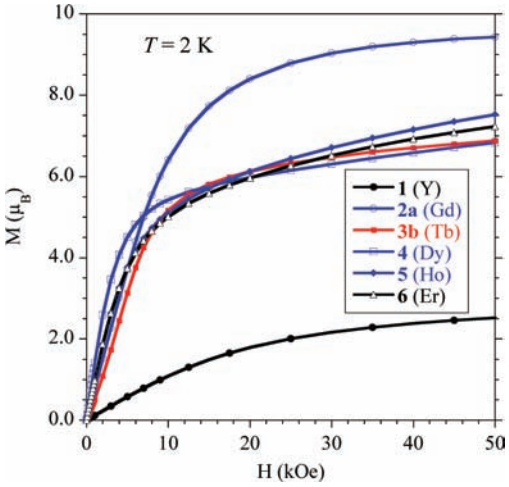

Figure 7. Field dependence of the magnetization recorded at 2 K (solid lines are only to guide the eye).

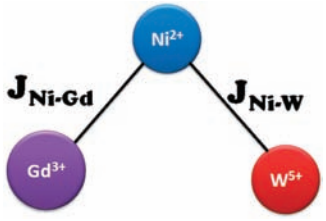

Figure 8. Schematic of {WNiGd} cluster (**2b**). The W^{5+}, Ni^{2+}, and Gd^{3+} ions correspond to site spins 1/2, 1, and 7/2, respectively. Exchange interactions J_{NiGd} and J_{NiW} are also shown.

octahedral surrounding (vide infra); the anisotropy of the Tb, Dy, Ho, and Er ions contributing further for **3a**,**b**, **4**, **5**, and **6**. Finally, it can be mentioned that not obvious differences are found for the $\chi_M T$ versus T and M versus H behaviors for the two Tb derivatives **3a** and **3b** (Figure 6,7, and Supporting Information).

Modeling. The magnetic property of {Ni−W−Gd} cluster **2a** has been modeled using the spin Hamiltonian for exchange interactions between the spins on Ni(II) and Gd(III) sites, as well as Ni(II) and W(V) sites (Figure 8), as the unperturbed Hamiltonian (eq 1) and using terms due to the external magnetic field along the z-direction, weak intermolecular exchange interaction, and a diagonal anisotropy term on the Ni(II) site as perturbations (eq 2). Since Gd(III) ion has $4f^7$ electron configuration the total orbital angular momentum is zero and single ion anisotropy due to spin−orbit interaction is taken to be absent. Similarly, W(V) has a lone unpaired electron spin and does not possess single ion anisotropy.

$$\check{H} = -J_{Ni-Gd}\hat{S}_{Ni}\cdot\hat{S}_{Gd} - J_{Ni-W}\hat{S}_{Ni}\cdot\hat{S}_{W} \qquad (1)$$

$$H' = g\mu_B H\sum_{i=1}^{3}\hat{S}_i^z - zJ'\langle\hat{S}_z\rangle\sum_{i=1}^{3}\hat{S}_i^z + D_{Ni}(\hat{S}_{Ni}^z)^2 \qquad (2)$$

where, J_{NiGd} (J_{NiW}) in eq 1 represents the exchange coupling between the Ni and Gd (W) spins and $\hat{S}$'s are the corresponding spin operators. A positive J_{NiGd} (J_{NiW}) corresponds to ferromagnetic exchange interaction between Ni(II) and Gd(III) (W(V)) ions (Figure 8). In this

(28) Shiga, T.; Ito, N.; Hidaka, A.; Okawa, H.; Kitagawa, S.; Ohba, M. *Inorg. Chem.* **2007**, *46*, 3492–3501.
(29) Sutter, J.-P.; Kahn, M. L.; Kahn, O. *Adv. Mater.* **1999**, *11*, 863–865.
(30) Kahn, M. L.; Sutter, J.-P.; Golhen, S.; Guionneau, P.; Ouahab, L.; Kahn, O.; Chasseau, D. *J. Am. Chem. Soc.* **2000**, *122*, 3413–3421.
(31) Sutter, J.-P.; Kahn, M. L. Lanthanide ions in molecular exchange coupled systems. In *Magnetism: molecules to materials*; Miller, J. S., Drillon, M., Eds.; Wiley-VCH: Weinheim, 2005; Vol. 5, pp 161−188.

system, the Ni(II) ion corresponds to spin 1 and W(V) to spin 1/2, while Gd(III) ion has spin 7/2.

To model magnetism in **2a**, we exactly solve the unperturbed exchange spin Hamiltonian (eq 1) in a chosen basis and obtain the energy eigenvalues $E_0(S,M_S)$. We then treat the Zeeman term, the intermolecular interaction, and the diagonal anisotropy terms as perturbations and compute the magnetic susceptibility. The first term in eq 2 is the Zeeman term while the second term corresponds to the intermolecular interactions. The parameter J' is the strength of intermolecular interaction and z is the number of nearest neighbors. Since Ni(II) ion is anisotropic, we have also introduced magnetic anisotropy, D_{Ni}, on the Ni ion, and this corresponds to the last term of the perturbation Hamiltonian H'. We obtain the molar magnetic susceptibility χ_M using the relations

$$\chi_M = \frac{N_A \mu_B^2 g^2 F(J,T)}{[k_B T - zJ' F(J,T)]} \quad (3)$$

$$F(J,T) = \frac{\sum_S \sum_{M_S=-S}^{+S} M_S^2 e^{-E(S,M_S)/k_B T}}{\sum_S \sum_{M_S=-S}^{+S} e^{-E(S,M_S)/k_B T}} \quad (4)$$

where, N_A is the Avogadro constant, μ_B is the Bohr magneton, g is gyromagnetic ratio, k_B is the Boltzmann constant, and $E(S,M_S) = E_0(S,M_S) + D_{Ni} M_{S_{Ni}}{}^2$.[1] Using these relations, we obtain the theoretical $\chi_M T$ as a function of temperature and fit it to the experimental data (Figure 6). The best fit to the experimental magnetic data corresponds to the parameter values, $J_{NiGd} = 2.17\ cm^{-1}$; $J_{NiW} = 27.1\ cm^{-1}$; $zJ' = -0.06\ cm^{-1}$; $g = 2.0$; $D_{Ni} = 0.5\ cm^{-1}$.

To confirm the strength of exchange interaction between the Ni and W sites, we have modeled the magnetic property of {Ni−W−Y} system **1** in which the Gd^{3+} ion is substituted by diamagnetic Y^{3+} ion. The exchange and perturbation Hamiltonians for this system are given by

$$\check{H} = -J_{Ni-W} \hat{S}_{Ni} \cdot \hat{S}_W \quad (5)$$

$$H' = g\mu_B H \sum_{i=1}^{2} \hat{S}_i^z - zJ' \langle \hat{S}_z \rangle \sum_{i=1}^{2} \hat{S}_i^z + D_{Ni} (\hat{S}_{Ni}^z)^2 \quad (6)$$

Using the method discussed above, we have obtained the exchange constants by fitting the magnetic susceptibility data (Figure 5). The best fit parameters for **1** are $J_{Ni-W} = 28.5\ cm^{-1}$; $zJ' = -0.51\ cm^{-1}$; $g = 2.02$; $D_{Ni} = 0.44\ cm^{-1}$.

The exchange parameters obtained are in good agreements with reported results. The {Ni−Gd} exchange interaction occurring in **2a** is very similar to the one found for the corresponding $\{L^{Me2}NiGd(NO_3)_3\}$ compound.[26] The smaller J parameter for **2a** is in line with the larger dihedral angle defined by the ONiO and OLnO planes of the bridging network, as in Cu−Gd complexes.[32] Indeed, it has been remarked that, mainly in Cu−Gd complexes,

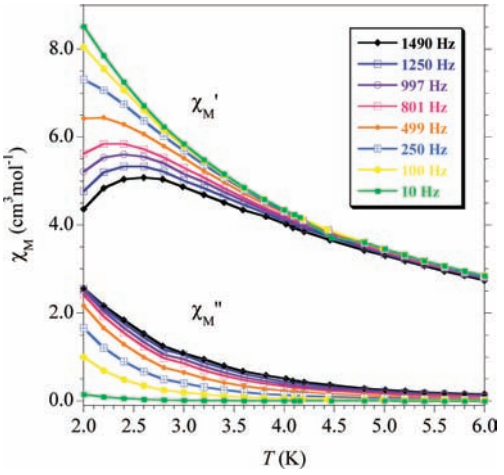

Figure 9. Frequency dependence of the real, χ_M', and imaginary, χ_M'', components of the AC-susceptibility for **3a** measured in $H_{ac} = 3$ Oe in the absence of static field.

there was a relation between the dihedral angle defined as the angle between planes involving the two bridging oxygen atoms and each metal ion, CuOO and GdOO planes, and the strength of the interaction parameter J. The larger J values are obtained when the CuOOGd core is planar (dihedral angle of 0°) and these values decrease when the dihedral angle increases.[32] This remark would mean that the 5d Gd orbitals, supposed to be unoccupied, would have a role in the interaction with the 3d orbitals of copper. This has been clearly explained by Cimpoesu, Hirao, et al. on the basis of modeling.[33] These authors demonstrate that the 5d orbitals are partially occupied and that the orthogonality of these 3d and 5d orbitals would be responsible for the ferromagnetic Cu−Gd coupling. Lowering the symmetry (increasing the dihedral angle) explains the antiferromagnetic exceptions (decreasing J values). The same argument may apply for the {Ni−Gd} pair.

For the octacyanometallates, it has been shown that the spin distribution and hence the exchange coupling are significantly influenced by the actual geometry of the $\{M(CN)_8\}$ unit.[20,34] The Ni−W interaction parameter found here for **1** and **2a** are well within the range of what is anticipated for a $\{W(CN)_8\}$ unit with square antiprism geometry.[13,20]

Dynamic Magnetic Susceptibility. A series of alternating current (AC) susceptibility studies have been undertaken for the Tb, Dy, Ho, and Er derivatives. As mentioned above, these anisotropic Ln ions may lead to slow relation dynamics of the magnetization, a signature of which is found in the imaginary part, χ_M'', of the AC susceptibility signal.[35] The temperature dependence of χ_M' and χ_M'' for **3a,b** (Figure 9 and 10) reveal frequency dependence for both the compounds but with noticeable differences. For **3b** the χ_M'' curves exhibit a maximum above 2 K for frequencies higher than 250 Hz, whereas no maxima are found for **3a**. For compound **4** only the onset

(32) Costes, J.-P.; Dahan, F.; Dupuis, A. *Inorg. Chem.* **2000**, *39*, 165–168.

(33) Paulovic, J.; Cimpoesu, F.; Ferbinteanu, M.; Hirao, K. *J. Am. Chem. Soc.* **2004**, *126*, 3321–3331.

(34) Pinkowicz, D.; Podgajny, R.; Nitek, W.; Makarewicz, M.; Czapla, M.; Mihalik, M.; Balanda, M.; Sieklucka, B. *Inorg. Chim. Acta* **2008**, *361*, 3957–3962.

(35) Gatteschi, D.; Sessoli, R. *Angew. Chem., Int. Ed.* **2003**, *42*, 269–297.

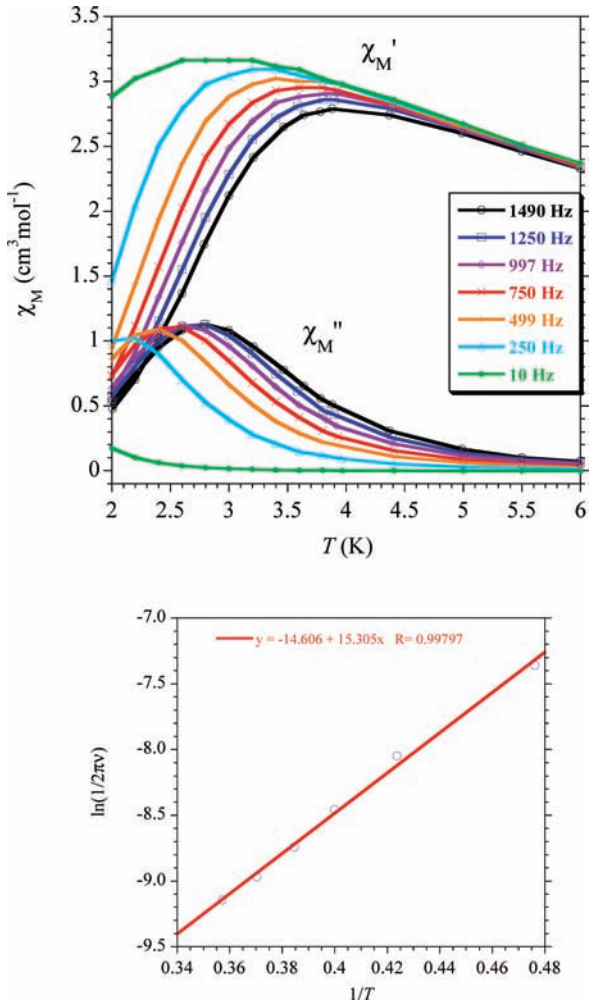

Figure 10. (top) Frequency dependence of the real, χ_M' and imaginary, χ_M'' components of the AC-susceptibility for $[L^{Me2}NiTb\{W(CN)_8\}]$ **3b** measured in $H_{ac} = 3$ Oe in the absence of static field. (bottom) Plot of $\ln(\tau)$ versus $1/T_B$; the straight line is the best fit to the data points.

of an out-of-phase signal is seen above 2 K, which precludes any conclusion about possible SMM-type behavior (see Supporting Information). For compounds **5** and **6** the χ_M'' responses do not deviate from zero down to 2 K.

At first glance, the difference of AC behavior for Tb derivatives **3a** and **3b** is striking. Both complexes exhibit very similar molecular structures with the same O-ligand surrounding for the Ln ions; replacing a dmf for a H_2O unit is not expected to significantly affect the ligand field. Moreover, for each compound the shape of the Ln coordination sphere is a distorted biaugmented trigonal prism (see SHAPE analysis in Supporting Information). It has been suggested that the symmetry of the ligand field may modulate the type of anisotropy exhibited by Tb, easy-axis anisotropy being related to low symmetry whereas easy-plane anisotropy is favored by more symmetrical environment.[12] Such a modulation cannot be excluded here even if occurrence of easy-axis type anisotropy for the Tb ions is supported by the low molecular symmetry, and evidenced by the AC behaviors for **3a** and **3b**. A more probable origin for the difference of dynamic susceptibility behavior is the crystal packing, which is notably different for the two compounds (see Supporting Information). For instance, considering the W−Ni axes (roughly the *z*-axis of the coordination sphere for Ni), the molecule arrangement leads to an angle of 56.9° between these axes for **3a** whereas this angle is of 66.9° for **3b**. Moreover, the molecules are not coplanar (plane containing the three ions), two types of layers are found with angles of 23.9° and 10.3° between them, respectively for **3a** and **3b**. Considering that the molecule-based magnetic moments have a preferred orientation, their relative positioning in the crystal will directly affect the macroscopic out-come. Unfortunately for the Ln ions, there is not obvious geometric parameter that permits to estimate the easy-axis orientation to further discuss this hypothesis.

The maxima of χ_M'' for different frequencies were used to determine the relaxation rate for **3b**.[36] The variation of $\ln(1/(2\pi\nu))$ with $1/T_B$, where T_B was taken as the temperature at the maximum of the χ_M'' curve for a given frequency (ν), is linear (Figure 10). The analysis of this curve by the Arrhenius equation $\tau = \tau_0 \exp(U_{eff}/k_BT)$, where τ represents the relaxation time and U_{eff} the effective energy barrier for spin reversal, yielded $\tau_0 = 4.5 \times 10^{-7}$ s and $U_{eff}/k_B = 15.3$ K in agreement with a SMM type behavior. It can be mentioned that the parent compound $\{L^{Me2}NiTb(NO_3)_3\}$, with a spin ground state smaller by just 1/2 as compared to **3b**, does not exhibit a χ_M'' signal down to 2 K. Moreover, the energy for reversal of the magnetization obtained for **3b** is remarkably high as compared to the few trimetallic complexes with slow relaxation features involving Ni and Tb or Dy that have been reported.[37,38]

Concluding Remarks. Assembling bimetallic $\{Ni-Ln\}^{3+}$ units and $\{W(CN)_8\}^{3-}$ is shown to be an efficient route toward heteronuclear {3d-4f-5d} compounds. Here the use of a coordinating solvent led to the formation of the smallest possible representatives, that is, trimetallic {NiLnW} derivatives. For all the compounds ferromagnetic {Ni−W} and {Ni−Ln} (Ln = Gd, Tb, Dy, Er) interactions are operative resulting in high-spin ground states. Parameterization of the magnetic behaviors for the Y and Gd derivatives confirmed the strong cyano-mediated {Ni−W} interaction (J_{NiW} = 27.1 and 28.5 cm^{-1}) compared to the {Ni−Gd} interaction (J_{NiGd} = 2.17 cm^{-1}).

One of the objectives of this investigation was to extend the SMM-type features to higher temperatures for {3d-4f} moieties involving anisotropic Ln ions. The behavior exhibited by one Tb derivative (U_{eff}/k_B = 15.3 K and $\tau_0 = 4.5 \times 10^{-7}$ s) validates the envisioned approach. The addition of a spin $S = 1/2$ (i.e., the W unit) in strong ferromagnetic interaction with the bimetallic {NiTb} has permitted to shift the blocking temperatures above 2 K. However, the incidence of the crystal phase on the observed dynamic susceptibility behavior is highlighted by the two Tb derivatives. At this stage it is not possible to

(36) Aubin, S. M. J.; Sun, Z.; Pardi, L.; Krzystek, J.; Folting, K.; Brunel, L.-C.; Rheingold, A. L.; Christou, G.; Hendrickson, D. N. *Inorg. Chem.* **1999**, *38*, 5329–5340.
(37) Pointillart, F.; Bernot, K.; Sessoli, R.; Gatteschi, D. *Chem.—Eur. J.* **2007**, *13*, 1602–1609.
(38) Chandrasekhar, V.; Pandian, B. M.; Boomishankar, R.; Steiner, A.; Vittal, J. J.; Houri, A.; Clérac, R. *Inorg. Chem.* **2008**, *47*, 4918–4929.

Table 1. Crystallographic Data

compound	**2b**	**3a**	**3b**	**4**	**5**	**6**
empirical formula	$C_{44.5}H_{63.5}GdN_{14.5}NiO_{11}W$	$C_{45.5}H_{62.5}N_{15.5}Ni_1O_{9.5}Tb_1W_1$	$C_{38}H_{52}N_{13}Ni_1O_{10.5}Tb_1W_1$	$C_{44}H_{61}Dy_1N_{15}Ni_1O_{10}W_1$	$C_{44}H_{59}Ho_1N_{15}Ni_1O_9W_1$	$C_{39.5}H_{54.5}Er_1N_{13.5}Ni_1O_{10.5}W_1$
formula weight	1377.41	1380.08	1260.40	1365.12	1349.54	1296.27
temperature	180 K	180 K	180 K	180 K	180 K	180 K
crystal system	monoclinic	monoclinic	monoclinic	monoclinic	monoclinic	monoclinic
space group	*Cc*	$P2_1/c$	$P2_1/c$	$P2_1/c$	$P2_1/c$	$P2_1/c$
unit cell dimensions	a = 22.6930(4) Å b = 10.9040(2) Å c = 22.1400(4) Å β = 95.256(2)°	a = 11.904(1) Å b = 25.841(2) Å c = 19.803(2) Å β = 106.362(2)°	a = 13.958(2) Å b = 15.064(1) Å c = 25.284(5) Å β = 94.12(1)°	a = 11.8310(6) Å b = 26.538(2) Å c = 19.745(1) Å β = 106.989(3)°	a = 12.0236(4) Å b = 26.0618(8) Å c = 19.6674(6) Å β = 106.467(1)	a = 13.8860(4) Å b = 15.0170(6) Å c = 25.593(1) Å β = 94.233(2)
volume	5455.4(2) Å^3	5844.8(8) Å^3	5303(3) Å^3	5928.9(6) Å^3	5910.1(3) Å^3	5322.2(3) Å^3
density	1.677	1.56826	1.579	1.529	1.515	1.618
absorption coefficient	3.715 mm^{-1}	3.541 mm^{-1}	3.896 mm^{-1}	3.558 mm^{-1}	3.541641 mm^{-1}	4.131 mm^{-1}
F(000)	2744	2748	2460	2704	2676	2536
Theta range for data collection	2.7−26.4°	1.3−26.3°	2.1−26.0°	1.3−28.7°	1.3−28.7°	1.6−34.8°
reflections collected	20555	54522	52783	76096	70157	89146
independent reflections	9651 [R(int) = 0.036]	11775 [R(int) = 0.053]	10360 [R(int) = 0.060]	13218 [R(int) = 0.041]	15205 [R(int) = 0.047]	22349 [R(int) = 0.041]
data/restraints/parameters	9651/8/660	8312/0/660	7293/5/564	7679/0/528	10836/8/629	14878/18/549
goodness-of-fit	1.005	1.0967	1.0850	1.0008	1.1236	1.1772
refinement on	F^2	F	F	F	F	F
final R indices [$^a I > 2\text{sigma}(I)$; $^b I > 3.0\backslash\text{s}(I)$]	R = 0.0241, wR = 0.0564[a] R_{all} = 0.0260, wR2 = 0.0572	R = 0.0316, wR = 0.0321[b]	R = 0.0421, wR = 0.0489[b]	R = 0.0778, wR = 0.0690[a]	R = 0.0333, wR = 0.0315[b]	R = 0.0412, wR = 0.0421[b]
largest diff. peak and hole	1.139 and −1.564 e Å^{-3}	1.48 and −0.56 e Å^{-3}	1.70 and −1.74 e Å^{-3}	4.17 and −3.29 e Å^{-3}	1.02 and −1.49 e Å^{-3}	1.80 and −2.84 e Å^{-3}

conclude if the origin of the differences found result from crystal packing or from subtle geometric consideration for the Ln coordination sphere. For the same reason and because of the structural variations for the series of compounds described here, comparison of the SMM performances as a function of the Ln ion is delicate. Nevertheless considering the three isomorphous compounds **3a**, **4**, and **5**, it appears that the trend Tb > Dy > Ho applies for the blocking temperatures.

Following this strategy, we are currently investigating the possibility of forming {3d-4f-5d} assemblages of larger nuclearity.

Experimental Section. The reagents $[(NHBu_3)_3\{W(CN)_8\}]$,[39] $[L^{Me2}Ni(H_2O)_{1.75}]$,[27,40] and $[L^{Me2}Ni(H_2O)_2\{Ln(NO_3)_3]$[26] have been prepared as described. Dry DMF was obtained on molecular sieves (4 Å), and THF was used as received. Magnetic measurements down to 2 K were carried out with a Quantum Design MPMS-5S SQUID susceptometer. The molar susceptibility was corrected for sample holder and for the diamagnetic contribution of all the atoms by using Pascal's tables.[1] All the measurements have been performed on crushed crystals from freshly isolated samples to avoid solvent loss by the crystals; the powders were mixed to grease. IR spectra were recorded on neat samples with a Perkin-Elmer *Spectrum 100* FT-IR spectrometer.

Synthesis. $[L^{Me2}Ni(dmf)Ln(dmf)_4\{W(CN)_8\}]\cdot H_2O$: 1 (Y), 2a (Gd), 3a (Tb), 4 (Dy), 5 (Ho). General Procedure. $L^{Me2}Ni(H_2O)_{1.75}$ (0.1 mmol; 48 mg) and $Ln(NO_3)_3\cdot 5H_2O$ (0.1 mmol) were mixed in dry DMF (5 mL). Upon dissolution, $(NHBu_3)W(CN)_8$ (0.1 mmol; 102 mg) was added. The reaction mixture was then layered with THF (5 mL) and left undisturbed. Amber-brown crystals were formed in the reaction tube after a few days. These were collected, washed with dmf and thf, and dried in air yielding the trimetallic species in nearly quantitative amounts. Analyses calculated (found) for $C_{44}H_{61}LnN_{15}NiO_{10}W$: **1** (Y): C, 40.92 (40.90); H, 4.76 (4.72); N, 16.26 (16.23); **2a** (Gd): C, 38.86 (38.74); H, 4.52 (4.74); N, 15.45 (15.30); **3a** (Tb): C, 38.81 (38.73); H, 4.51 (5.0), N, 15.43 (15.32); **4** (Dy with 1dmf less): C, 38.11 (37.78); H, 4.21 (4.41), N, 15.18 (14.94); **5** (Ho, + 1 H_2O): C, 38.14 (38.06); H, 4.58 (4.22); N, 15.16 (14.84). IR (selected bands common to all derivatives, cm^{-1}): 2169 (v), 2142 v), 1638 (s), 1462 (m), 1434 (m), 1375 (s), 1070 (m), 743 (m), 675 (s). Cell parameters determined at 180 K for **1**: a = 11.99 b = 25.79 c = 19.84 β = 106.70°, V = 5878 Å^3.

$[L^{Me2}Ni(dmf)Gd(dmf)_3(H_2O)\{W(CN)_8\}]\cdot H_2O\cdot 0.5THF\cdot 0.5$ dmf, 2b. $L^{Me2}Ni(H_2O)_{1.75}$ (0.1 mmol, 48 mg) and $Gd(NO_3)_3\cdot 6H_2O$ (0.1 mmol, 49 mg) were dissolved in a mixture of dmf (6 mL) and H_2O (1 mL) followed by the addition of $(NHBu_3)W(CN)_8$ (0.1 mmol; 102 mg). The resulting solution was then layered with THF (3 mL) and left undisturbed for diffusion. After one week well shaped purple crystals of **2b** (72 mg, Y = 52%) were isolated by decantation. Analysis calculated (found) for $C_{44.5}H_{63.5}GdN_{14.5}NiO_{11}W$: C, 38.80 (39.02); H, 4.64 (4.54); N, 14.74 (14.89). IR (selected bands, cm^{-1}): 3245 (w broad), 2939 (m broad), 2185 (w), 2161 (w), 2144 (w), 1637 (s), 1464 (m), 1432 (m), 1375 (m), 1296 (m), 1222 (m), 735 (m), 673 (m).

$[L^{Me2}Ni(H_2O)Tb(dmf)_{2.5}(H_2O)_{1.5}\{W(CN)_8\}]\cdot H_2O\cdot 0.5dmf$, 3b. As for **3a** but with technical grade dmf. Analysis calculated (found) for $C_{38}H_{52}N_{13}NiO_{10.5}TbW$: C, 36.26 (36.38); H, 4.16 (4.16); N, 14.45 (14.33). IR (selected bands, cm^{-1}): 3400 (broad), 2940 (m), 2130 (v), 2161 (v), 2144 (v), 1652 (s), 1468 (m), 1438 (m), 1377 (m), 1297 (m), 1224 (m), 1067 (m)

$[L^{Me2}Ni(H_2O)Er(dmf)_3(H_2O)\{W(CN)_8\}]\cdot H_2O\cdot 0.5dmf$, 6. $L^{Me2}Ni(H_2O)_{1.75}$ (0.1 mmol, 48 mg), $(NHBu_3)W(CN)_8$ (0.1 mmol; 102 mg), and $Er(NO_3)_3\cdot 6H_2O$ (0.1 mmol, 44 mg) were dissolved in technical grade dmf (4 mL) and layered with THF (5 mL). Slow solvent interdiffusion over a period of 3 weeks yielded small orange crystals of **6**. Analysis calculated (found) for $C_{39.5}H_{54.5}N_{13.5}NiO_{10.5}ErW$: C, 36.60 (36.38); H, 4.24 (4.16); N, 14.59 (14.33). IR (selected bands, cm^{-1}): 3460 (w, broad), 2938 (w, broad), 2182 (w), 2162 (w), 2146 (w), 2128 (w), 1642 (s), 1475 (m), 1460 (m), 1435 (m), 1373 (m), 1294 (m), 1069 (m), 741 (m), 682 (m).

X-ray Diffraction. Intensity data were collected at 180 K on an Xcalibur Oxford Diffraction (**2b**), on an IPDS Stoe (**3b**), or an Apex2 Bruker (**3a, 4, 5,** and **6**) diffractometer using a graphite-monochromated Mo Kα radiation source and equipped with an Oxford Cryosystems Cryostream Cooler Device with liquid nitrogen cooler devices (and an Oxford Instrument Cooler Device for **2b**, and an Oxford Cryosystems Cryostream Cooler Device for **3a,b** and **4**).

The structural determination for **2b** was carried out by direct methods using SIR92[41] and the refinement of atomic parameters based on full-matrix least-squares on F^2were performed using the SHELX-97 programs[42] within the WINGX package.[43] The structure of **2b** has been solved with one THF and one dmf with partial occupation (1/2), the positions O20A and C54B being shared by the two molecules. The structures **3a,b, 4, 5**, and **6** have been solved by Direct Methods using SIR92,[41] and refined by least-squares procedures on F using the program Crystal running on a PC.[44] Hydrogen atoms were refined using a riding model. For **3a** all coordinated dmf molecules and non-hydrogen atoms have been refined anisotropically. For **3b** one of the depicted dmf bound to Tb has occupation 1/2, the O6 being common with H_2O found when the dmf is absent; a second dmf linked to Tb has one of the C atoms disordered over two positions (C321, C322). For compound **5**, all non-hydrogen atoms were refined anisotropically. Two of the coordinated dmf molecules are partly disordered. Water molecules in the crystal lattice appear to be highly disordered, and it was difficult to model reliably their positions and distribution. Therefore, the SQUEEZE function of PLATON[45] was used to eliminate the contribution of the electron density in the solvent region from the intensity data, and the solvent free model was employed for the final refinement. Chemical analysis for this compound suggests the occurrence of two lattice H_2O molecules per trinuclear unit. For compound **6**, all the atoms of the molecular complex have been refined anisotropically, except the disordered moieties of the coordinated dmf molecules.

Results are summarized in Table 1.

Acknowledgment. This work was supported by the Centre Franco-Indien pour la Promotion de la Recherche Avancée/Indo-French Centre for the Promotion of Advanced Research (CEFIPRA/IFCPAR Project 3108-3) and by the European Union sixth framework program NMP3-CT-2005-515767 entitled "*MAGMANet: Molecular Approach to Nanomagnets and Multifunctional Materials*". Work carried out in Bangalore was also supported by DST, India through the research Grant SR/S1/IC-08/2008. The authors are grateful to Dr. A. Mari, M. L. Réchignat, M. A. Moreau, and Ms. S. Seyrac for technical assistance.

(39) Dennis, C. R.; van Wyk, A. J.; Basson, S. S.; Leipoldt, J. G. *Transition Met. Chem.* **1992**, *17*, 471–473.
(40) Pfeiffer, P.; Breith, E.; Lülle, E.; Tsumaki, T. *Justus Liebigs Ann. Chem.* **1933**, *503*, 83.
(41) Altomare, A.; Cascarano, G.; Giacovazzo, C.; Guagliardi, A. *J. Appl. Crystallogr.* **1993**, *26*, 343–350.
(42) Sheldrick, G. M. *Programs for Crystal Structure Analysis*, Release 97−2; University of Göttingen: Göttingen, Germany, 1998.
(43) Farrugia, L. J. *J. Appl. Crystallogr.* **1999**, *32*, 837.
(44) Betteridge, P. W.; Carruthers, J. R.; Cooper, R. I.; Prout, K.; Watkin, D. J. *J. Appl. Crystallogr.* **2003**, *36*, 1487.
(45) Spek, A. L. *PLATON, A Multipurpose Crystallographic Tool*; Utrech University: Utrecht, The Netherlands, 2001.

Supporting Information Available: X-ray crystallographic file in CIF format for **2b**, **3b**, **4**, **5** and **6**; ORTEP plots with numbering scheme; results of SHAPE analyses; $\chi_M T$ versus T and M versus H behaviors for **3a**, AC susceptibility plots for **4**. This material is available free of charge via the Internet at http://pubs.acs.org.